Atomic Dimer Shuttling and Two-Level Conductance Fluctuations in Nb Nanowires

Alexei Marchenkov, Zhenting Dai, Chun Zhang, Robert N. Barnett, and Uzi Landman

School of Physics, Georgia Institute of Technology, Atlanta, Georgia 30332, USA
(Received 10 October 2006; published 22 January 2007)

We present high-resolution conductance measurements in niobium nanowires below the superconduct-ing transition temperature. During elongation we find a bistability region manifesting itself as random telegraph noise. Density functional structural optimizations and conductance calculations reproduce and explain the measurements. In particular, the observed bistability is associated with the formation of a niobium dimer between the opposing electrodes, with the dimer shuttling between a symmetric, high conductance, and an asymmetric, low-conductance configurations in the gap.

The structural, mechanical and electronic properties of nanowires (NWs) suspended between opposing electrodes have been the subject of continued interest and discovery [1] since the early description of the formation of metallic NWs generated through elongation of a contact between a Ni tip and an Au surface [2]. In the early studies, and in subsequent work [1,3–6], it has been shown that the elon-gation of a NW proceeds through alternating stages of stress accumulation during which the atomic structure de-forms elastically, and stress relief, or yield, involving fast structural rearrangement, that are portrayed in both the force and electrical conductance data recorded during the elongation process. In the force profiles plotted versus the separation distance these elongation stages are reflected in sawtooth oscillations, and in the conductance records they appear as quantized conductance plateaus separated by jumps of the order of the conductance quantum ($G_0 \equiv 2e^2/h = 1/12\,906\ \Omega^{-1}$), or multiples thereof. This is in accord with the Landauer theory [7] where the total con-ductance is given by $G = G_0 \sum_{j=1}^{N} \tau_j$ with $\{\tau_j\} \equiv \{\tau_1, \ldots, \tau_N\}$ denoting the set of transmission coefficients of the N channels that contribute to the NW conductance at a given NW configuration. The channel composition $\{\tau_j\}$ can be deduced from low-voltage IV characteristics of atomic-size superconducting point contacts or NWs [8–12].

It has been predicted theoretically and shown experi-mentally [1–6,13] that indeed the structural and transport properties of NWs are correlated with each other, and that precisely at conductance jumps between neighboring pla-teaus fluctuations may occur in the form of random tele-graph noise (RTN), involving high and low-conductance states (HG and LG, respectively), whose origin remains unknown [14,15]. However, short of direct imaging of the NW structure during elongation and simultaneous conduc-tance measurements [16], evidence for the aforementioned close correlation between the structural and transport char-acteristics is lacking.

Here we report on experimental and theoretical studies of niobium contacts in the final stages before breakup,

when the conductance is of the order of 2–4G_0 with a few contributing channels. We present experiments per-formed on microfabricated mechanically-controlled break junctions (MCBJ) in a cryogenic setup that permits very high levels of stability and control over the elongation process. Analysis of data obtained during reversible ma-nipulation of the contacts below [9–11] and above the superconducting transition temperature, allowed determi-nation of the conductance channel compositions at various stages of the elongation process, including a switching stage where two-level RTN is observed. The use of density functional theory (DFT) electronic structure calculations, coupled with structural optimizations and evaluations of the electric conductance [using the nonequilibrium Green's functions (NEGF) method [17,18]] allowed us to deter-mine that the NW structure underlying, and consistent with, the complete set of experimental observations, con-sists of a Nb dimer suspended between the two electrodes. The calculated conductance variations as a function of elongation, reversibility, patterns revealed in the channel composition, and two-level switching behavior between HG and LG states corresponding to symmetric and asym-metric positions of the dimer in the gap (with the latter one predominating for larger gap widths), faithfully reproduce the experimental observations.

As mentioned above, we used microfabricated samples in a cryogenic MCBJ setup, prepared by dc-magnetron sputtering of Nb onto a 1 μm thick insulating polyimide layer covering a flexible bronze substrate [11]. The proce-dure was optimized for producing high superconducting transition temperatures, which tends to yield microcrystal-line thin films [19]. Scanning electron micrographs of samples previously used in our experiments indicate that breaking occurs by cleaving along the boundary between two microcrystallites. Our MCBJ setup yields remarkably stable contacts and allows reversible manipulation within an ~1 Å elongation range. We could restore the length of the contact with an accuracy better than 1 pm and repro-duce highly nonlinear IV and conductance (dI/dV) char-acteristics, even after several hours of experimentation. All

measurements reported here were performed in ultrahigh vacuum conditions at 4.2 and 9 K.

We started by adjusting the contacts' conductance to just below $\sim 3G_0$ using a coarse screw actuator. This conductance corresponds to the most probable atomic configuration as can be judged from the conductance histogram obtained using notched-wire samples [10]. From this point, we used the fine piezoactuator. After adjusting the length, we measured the contact's current-voltage (IV) and conductance (dI/dV) characteristics and determined the channel composition. Typical behavior seen in 18 contact realizations from 5 different samples is as follows: as the contact was stretched, the conductance gradually decreased to $(2.4 \pm 0.15)G_0$ [Fig. 1(a)]; subsequently, in an elongation range of ~ 0.1 Å we observed slow two-level fluctuations (with a conductance difference of up to $0.6G_0$) between well-defined HG and LG values, which showed characteristics of RTN [Figs. 1(d)–1(f)]; upon further elongation, the state with lower conductance was stabilized [Figs. 1(a) and 1(e)]. At any point the direction of the contact length adjustment could be reversed and the conductance behavior reproduced without detectable hysteresis. Elongation beyond the range shown in Fig. 1(a) results in breakup of the contact.

The conductance evolution curve shown in Fig. 1(a) includes multiple traversing of the RTN region, where the conductance was obtained by time averaging of the two-level fluctuations [Fig. 1(d) and 1(e)]. This behavior was reproduced both in the superconducting state, where the conductance is determined from dI/dV on the resistive branch ($eV > 2\Delta$, where Δ is the superconducting gap), and in the normal state at temperatures above our devices' superconducting transition temperature of ~ 8.8 K. It has been previously shown that suppression of superconductivity in aluminum atomic-size contacts by either raising the temperature or applying a magnetic field does not affect their electronic structure seen through the channel composition [20]. We have experimentally verified the temperature independence of our results for both the HG and LG states. Differential conductance curves of the HG and LG configurations taken in the vicinity of the RTN region are shown in Figs. 1(b) and 1(c); the corresponding IV curves are shown in Fig. 1(f). The most noticeable difference is that there are two high-transparency ($\tau_j \gtrsim 0.6$) channels in the HG state, while there is a single such channel in the LG state (see the inset in Fig. 1); for all experimental contact realizations it is the transparency of the latter channel that was higher than that of the highest-transparency channel of the HG state. This can be qualitatively seen from the higher conductance in the LG state near zero voltage bias [compare Figs. 1(b) and 1(c)].

Manipulation of the contact length in the RTN region allowed us to change the ratio of the time the NW spent in the two states [Figs. 1(d)–1(f)], which is consistent with
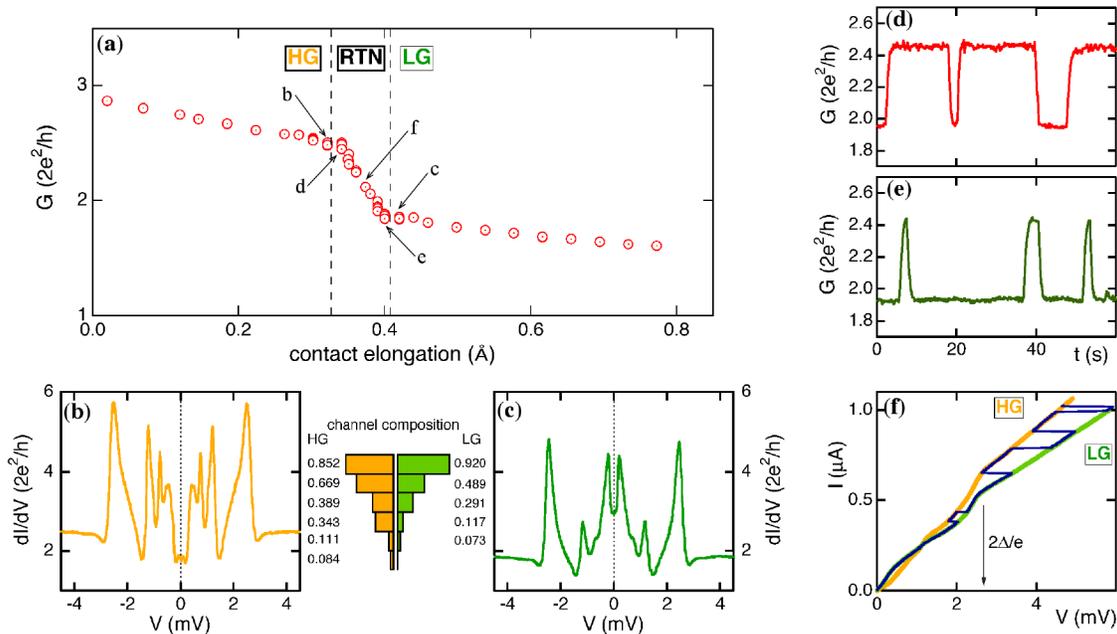
FIG. 1 (color online).   (a) Reversible variation of the conductance versus elongation distance recorded at 4.2 K. Similar results were obtained above the superconducting transition temperature. With further elongation the NW breaks. (b),(c) The differential conductance of the HG [(b), yellow online] and the LG [(c), green online] states versus voltage. The measurements correspond to points b and c in panel (a). The corresponding channel compositions are shown in the inset between (b) and (c). (d),(e) Temporal conductance fluctuations near the HG and LG states, respectively, taken at points d and e in panel (a). The contacts were current-biased at $I_{\text{bias}} = 0.75$ μA. (f) Switching between the two states recorded while acquiring the IV characteristics in the middle of the RTN region (solid line, blue online). The curves marked HG and LG (yellow and green online) correspond to the dI/dV curves shown in (b) and (c). The acquisition of each curve in (f) takes about two minutes.

adjusting the two minima in the double-well potential describing the fluctuating system [21,22].

Insights into the nature of bonding, atomic arrangements, structural transitions, and electronic transport in Nb nanowires formed upon the separation of the leads were obtained through DFT electronic structure calculations [23] and conductance calculations with the combination of DFT and the NEGF [17,18,24]. The DFT calculations include the generalized gradient approximation (GGA) [25], using a plane wave basis (kinetic energy cutoff $E_{cut} = 68$ Ry), and norm-conserving soft pseudopotentials [26,27].

We explored first the electronic and atomic structures of several atomic contacts and nanowire configurations spanning the gap between two opposing Nb electrodes of pyramidal shapes (Fig. 2). In structural optimizations all the Nb atoms included in the "contact region" [see Fig. 2(a)] are fully relaxed, while the other atoms (considered as part of the leads) are held in their bulk Nb lattice positions; we have found that changes in the distance between the electrodes express themselves essentially entirely in variations of distances in the gap region only. These relaxed local structures are subsequently used in the NEGF transport calculations which employ semi-infinite bcc (100) leads (consisting of bcc stacked alternating 4- and 5-atom layers) and the contact region [see Fig. 2(a)]. In the NEGF calculations we used an atomic

FIG. 2 (color online). Nb nanowire configurations and wave functions. (a) The division of the system into the contact region and the two leads. A symmetric Nb dimer is shown in the gap (i.e., $a = a'$). (b) A symmetric high-conductance (HG) configuration (left) and an asymmetric low-conductance (LG) one, both corresponding to $L_{gap} = 8.13$ Å. For both we show superimposed on the atomic structure isosurfaces of the highest (lowest) occupied (unoccupied) molecular orbitals, homo (lumo), respectively, with energies close to the Fermi level. The orbitals shown have large overlaps with the conductance eigenchannels. These Kohn-Sham wave functions are made predominantly of d-states and they extend over the Nb dimer and the leads. The two shades (blue and green online) correspond to positive and negative signs of the wave functions.

basis with the same 10 orbitals per atom as those used in the construction of the pseudo potential, which are then expanded in a plane wave basis with $E_{cut} = 68$ Ry.

Several configurations that we have explored initially yielded results that do not correspond to the experimental findings: most importantly, they do not show two-level behavior upon stretching of the contact. These include (i) the case of two electrodes sharing a common vertex atom (separated by the bulk nearest-neighbor distance, $d_{nn} = 2.66$ Å from the nearest atom in the underlying layer) yielding a conductance of $\sim 5G_0$ [28], and (ii) a configuration where the two electrode tips are bridged by a single suspended atom separated by d_{nn} from each of the tip atoms, with a conductance of $4.8G_0$. As we describe below, the only nanowire configuration whose transport and structural characteristics agree well with the measurements for the entire range of tip-to-tip gap distances, L_{gap}, discussed in this Letter, consists of a dimer of Nb atoms suspended in the gap between the opposing Nb electrodes (Fig. 2).

We begin with a gap width $L_{gap} = 7.6$ Å, where in equilibrium the two Nb nanowire atoms are separated by $d = 2.05$ Å, and their distances from the tip atoms $a = a' = 2.77$ Å. The calculated conductance for this configuration is $3.0G_0$, with a channel composition {0.92, 0.82, 0.48, 0.33, 0.24, 0.1}; we list only channels with $\tau_j \gtrsim 0.1$. This correlates well with the highest measured conductance value shown in Fig. 1. As long as $L_{gap} < 8.0$ Å only a symmetric [i.e., $a = a'$, see Fig. 2(b) left] dimer configuration is found to be stable, with the conductance decreasing slowly and monotonically upon stretching of the contact. However, when $L_{gap} = 8.13$ Å two states of the suspended Nb dimer are found: the lower energy one corresponds to a symmetric dimer, and the higher energy (0.4 eV) metastable isomer is a displaced asymmetric dimer configuration [i.e., $a' > a$, see Fig. 2(b), right]. The symmetric dimer structure with $d = 2.05$ Å, and $a = a' = 3.04$ Å is an HG state, $G = 2.6G_0$ and a channel composition {0.90, 0.81, 0.39, 0.16, 0.13}, and the asymmetric configuration (LG state) is a local energy minimum in the gap with $d = 2.06$ Å, $a = 2.52$ Å and $a' = 3.55$ Å, and it exhibits a lower conductance ($2.1G_0$) and a corresponding channel composition {0.91, 0.57, 0.30, 0.16, 0.12}. It is noteworthy that the close top two conductance channels ($0.90G_0$ and $0.81G_0$) in the symmetric HG dimer configuration, are split in the asymmetric LG isomeric, with the conductance being dominated by a single channel ($0.91G_0$); a similar trend is seen in the channel composition of the HG and LG states in the RTN region of the measurements [see inset between panels (b) and (c) in Fig. 1]. Two-level behavior is also found for an additional (short) stretching range (with a smaller energy difference between the two states).

Throughout the elongation process described above the structural variations of the NW and of the transport char-

acteristics are reversible. However, past a certain elongation the two-state characteristic behavior ceases, and only a single low-conductance state is found, corresponding to an asymmetric dimer. Continued stretching leads to breaking of the NW with the dimer remaining attached to one of the electrodes. This differs from the case of a gold dimer NW where upon breaking each of the dimer atoms sticks to a different electrode [29].

In Fig. 2(b) we display for the HG (symmetric dimer state, $G = 2.6G_0$) and LG (asymmetric dimer state, $G = 2.1G_0$) configurations of the Nb dimer, isosurfaces of wave functions (with energies near the Fermi energy) that are found to have large overlaps with the conductance eigenchannels [30]. The d character of the orbitals contributing to transport is evident, as well as their extended nature that connects the suspended NW atoms in the gap to the supporting electrodes and leads.

In summary, from measurements on microfabricated break junctions we found that the conductance of Nb nanowires shows upon elongation of the contact by less than 1 Å a reversible evolution from $G \approx 3G_0$ to $G \leq 2G_0$. This includes a narrow bistability region where temporal fluctuations between high and low-conductance states occur. Measurements in the superconducting state allowed determination of the channel composition as a function of the degree of elongation, revealing a change in the characteristics of the dominant conducting channels between the two states. These results are reproduced and explained by DFT calculations and structural optimizations coupled with conductance evaluations. In particular, we conclude that the nanowire consists of a Nb dimer suspended between atomically sharp contacts. The two-level telegraph noise characteristics originate from shuttling of the dimer between a symmetric (high-conductance) and asymmetric (low-conductance) configurations. In this manner, we have demonstrated that accurate nanowire manipulations and high-resolution conductance measurements, in conjunction with high level theoretical simulations, can serve as a reliable electronic transport spectroscopy and an atomic structure microscopy of nanowires and point contacts.

[1] N. Agraït, A. Levy Yeyati, and J. M. van Ruitenbeek, Phys. Rep. **377**, 81 (2003).
[2] U. Landman et al., Science **248**, 454 (1990).
[3] J. I. Pascual et al., Science **267**, 1793 (1995).
[4] U. Landman et al., Phys. Rev. Lett. **77**, 1362 (1996).
[5] G. Rubio et al., Phys. Rev. Lett. **76**, 2302 (1996).
[6] E. Scheer et al., Nature (London) **394**, 154 (1998).
[7] R. Landauer, Philos. Mag. **21**, 863 (1970).
[8] The total current-voltage (*IV*) characteristic is expressed as $I(V) = \sum_{j=1}^{N} i(V, \tau_j)$, where the independent $i(V, \tau_j)$ curves exhibit a series of sharp current steps at voltages $V = 2\Delta/ne$, corresponding to multiple Andreev (quasiparticle) reflections of order $n = 1, 2, \ldots$, and Δ is the superconducting gap. Fitting to the measured data is made by using $i(V, \tau_j)$ curves generated numerically for a dense set of channel transparencies τ_j through solution of the Bogoliubov-de Gennes equations (see Refs. [9,10]). For further details see Ref. [11].
[9] E. Bratus', V. Shumeiko, and G. Wendin, Phys. Rev. Lett. **74**, 2110 (1995); A. Ingerman et al., Phys. Rev. B **64**, 144504 (2001).
[10] B. Ludoph et al., Phys. Rev. B **61**, 8561 (2000).
[11] Z. Dai and A. Marchenkov, Appl. Phys. Lett. **88**, 203120 (2006).
[12] E. Scheer et al., Phys. Rev. Lett. **78**, 3535 (1997).
[13] C. Yannouleas et al., Phys. Rev. B **57**, 4872 (1998).
[14] C. J. Muller et al., Phys. Rev. Lett. **69**, 140 (1992).
[15] H. van den Brom et al., Physica (Amsterdam) **252B**, 69 (1998).
[16] H. Ohnishi et al., Nature (London) **395**, 780 (1998).
[17] J. Taylor et al., Phys. Rev. B **63**, 245407 (2001).
[18] M. Brandbyge et al., Phys. Rev. B **65**, 165401 (2002).
[19] J. Halbritter, J. Appl. Phys. **97**, 083904 (2005).
[20] E. Scheer et al., Physica (Amsterdam) **280B**, 425 (2000).
[21] M. B. Weissman, Rev. Mod. Phys. **60**, 537 (1988).
[22] A. Halbritter et al., Adv. Phys. **53**, 939 (2004).
[23] R. N. Barnett and U. Landman, Phys. Rev. B **48**, 2081 (1993).
[24] In the NEGF method we take the Hamiltonians in the two semi-infinite leads as bulklike. Then, the self energies, Σ_L and Σ_R, which describe the interactions between the left (*L*) and right (*R*) leads with the contact region [see Fig. 2(a)] and the Green's functions (retarded and advanced, $G^{r,a}$), can be calculated (see Refs. [17,18]). The transmission (as a function of energy) in the Landauer expression for the conductance can be evaluated as $T(\epsilon) = \mathrm{Tr}[\Gamma_L(\epsilon)G^r(\epsilon)\Gamma^R(\epsilon)G^a(\epsilon)]$, where $\Gamma^{L,R} = \Sigma_{L,R}^r - \Sigma_{L,R}^a$. For further details see C. Zhang et al. (to be published).
[25] J. P. Perdew et al., Phys. Rev. Lett. **77**, 3865 (1996).
[26] N. Troullier and J. L. Martins, Phys. Rev. B **43**, 1993 (1991).
[27] In the pseudopotential construction we used as a reference configuration $[\mathrm{Kr}]4s^2 4p^6 4d^5 5s^0$, i.e., 13 valence electrons per atoms as described in H. Grönbeck et al., Phys. Rev. A **58**, 4630 (1998). In this scheme the electronic configuration of the atom is given correctly to be $[\mathrm{Kr}]4s^2 4p^6 4d^4 5s^1$.
[28] A similar configuration but with one of the electrodes rotated about the *z* axis has been used in a self-consistent tight-binding NEGF calculation yielding a conductance of $\sim 2.9G_0$, see J. C. Cuevas et al., Phys. Rev. Lett. **80**, 1066 (1998).
[29] H. Hakkinen et al., J. Phys. Chem. B **104**, 9063 (2000).
[30] M. Brandbyge et al., Phys. Rev. B **56**, 14 956 (1997).